QUEEN'S UNIVERSITY BELFAST

Probing the environment of an inaccessible system by a qubit ancilla

Campbell, S., Paternostro, M., Bose, S., & Kim, M. S. (2010). Probing the environment of an inaccessible system by a qubit ancilla. *Physical Review A*, *81*(5), [050301]. https://doi.org/10.1103/PhysRevA.81.050301

Published in:
Physical Review A

Document Version:
Publisher's PDF, also known as Version of record

Queen's University Belfast - Research Portal:
Link to publication record in Queen's University Belfast Research Portal

Publisher rights
©2010 The American Physical Society

General rights
Copyright for the publications made accessible via the Queen's University Belfast Research Portal is retained by the author(s) and / or other copyright owners and it is a condition of accessing these publications that users recognise and abide by the legal requirements associated with these rights.

Take down policy
The Research Portal is Queen's institutional repository that provides access to Queen's research output. Every effort has been made to ensure that content in the Research Portal does not infringe any person's rights, or applicable UK laws. If you discover content in the Research Portal that you believe breaches copyright or violates any law, please contact openaccess@qub.ac.uk.

Download date:28. Mar. 2023

PHYSICAL REVIEW A **81**, 050301(R) (2010)

Probing the environment of an inaccessible system by a qubit ancilla

S. Campbell,[1] M. Paternostro,[1] S. Bose,[2] and M. S. Kim[1]
[1]*School of Mathematics and Physics, Queen's University, Belfast BT7 1NN, United Kingdom*
[2]*School of Physics and Astronomy, University College London, Gower Street, London WC1E 6BT, United Kingdom*
(Received 14 August 2009; published 11 May 2010)

We study the conditions for probing the environment affecting an inaccessible system by means of continuous interaction and measurements performed only on a probe. The scheme exploits the statistical properties of the probe at its steady state and simple data postprocessing. Our results, highlighting the roles played by interaction and entanglement in this process, are both pragmatically relevant and fundamentally interesting.

DOI: 10.1103/PhysRevA.81.050301 PACS number(s): 03.67.Mn, 03.65.Ud, 03.65.Yz

Examining the dynamics of a complex system is known to be difficult, also in light of the fact that direct access to its constituent parts may often be impossible. Built-in charge qubits embedded in superconducting waveguides, which can only be accessed through their electromagnetic field [1], electron spins in self-assembled quantum-dot arrays [2], the mechanical part of nanoelectromechanical systems and their optomechanical counterparts [3,4], single-molecule junctions [5], arrays of Josephson junctions with only a few of them coupled to read-out antennae, or cold quantum gases and optical lattices [6] are striking examples of the situation depicted here, where only partial access to the components of a complex and multipartite system is possible. In these instances, the use of ancillary probing devices represents a valuable diagnostic tool for the gain of information on inaccessible evolutions. First, the coupling to such ancillae is frequently the only way to grant some access, although indirect. Second, when unitary dynamics and fine time control are in order, special techniques of "interaction tomography" based on ancillae may be used [7]. Here we are interested in the case where the element to probe experiences a nonunitary evolution. The interesting question we assess is whether a proper characterization of such an open system is still possible and which are the crucial ingredients for such a process to be effective. Using a physically significant model where an ancilla is continuously coupled to the system to be probed and its steady state measured, we show that simple postprocessing enables the characterization of an open-system dynamics. In fact, current experiments have already realized all the necessary ingredients to implement the proposed scheme and their results can simply be reinterpreted to be exactly in line with our findings [8].

In addition to the above pragmatic interests, our central question is also fundamentally important. The ability to reliably determine the environmental parameters affecting inaccessible systems is vital in the development of means to control such spoiling effects. Quite strikingly, we show this can be done via the presence of an interaction with an ancillary system and, aside from the nature of the system to be probed, no other strong assumptions are made, making our scheme remarkably flexible and readily implementable. Interestingly, entanglement turns out to be inessential [9]. The presence of simple classical correlations is sufficient to reliably infer the main features of the system under scrutiny. In this respect, our study is different from others dealing with the revelation of the quantum correlations within a large environment by detecting entanglement generated between two independent probes [10]. Moreover, although the idea might be reminiscent of schemes for quantum nondemolition measurements, the underlying concepts are quite different. Instead of writing the information encoded in a specific degree of freedom of the system to be probed onto a "meter," here we show that one can operatively characterize a given evolution simply by looking at the spectrum of the statistical two-time correlations of the probe. We also stress the differences with a trivial ideal state-swapping operation: here we look at the steady state of a system in continuous interaction with its environment, which is what one should realistically expect to occur. In this respect, our proposal is also distinguished from any scheme relying on the quantum Zeno effect, which would require proper timing of measurements performed on the probing part [11].

We start by considering the simple case of two qubits, labeled 1 and 2 and characterized by the respective transition frequency ω_j $(j = 1,2)$. The free evolution of the qubits is ruled by the Hamiltonian $\hat{\mathcal{H}}_f = \frac{1}{2}\sum_{j=1}^{2}\omega_j\hat{\sigma}_{z,j}$ (we take $\hbar = 1$) with $\hat{\sigma}_k$ $(k = x,y,z)$ the k Pauli operator and $\{|g\rangle,|e\rangle\}$ the ground and excited state of each qubit. Qubit 2 embodies the system whose dynamics we want to characterize through the detection stage represented by qubit 1. To account for the case where qubit 2 is originally part of a multipartite register whose state we are not interested in, we allow for qubit 2 to be prepared in a general mixed state. This would be the case, for instance, when this qubit is originally entangled with the rest of a register. The second assumption we make is that qubit 1 is in a pure state, well isolated from the environment $\mathcal{B}$ affecting 2. This condition does not affect the generality of our results and can easily be relaxed. We also make no assumptions on the features of $\mathcal{B}$, although we assume its Markovian nature. Such a simplification allows the problem to be treated with a Liouvillian approach requiring the use of a standard "quantum optics" master equation (ME). It should be stressed that the validity of such an approach extends to quite a wide range of relevant physical settings [12]. We allow the qubits to interact via the coupling Hamiltonian $\hat{\mathcal{H}}$, whose choice is a setup-dependent issue. Its form is usually guided by naturally or easily realized interactions, specific to a chosen implementation. One could even consider the case where probe and system to be probed have different physical natures. As $\hat{\mathcal{H}}$ embodies one of the key tools in our scheme, we assume the ability to engineer the most suitable form of coupling, possibly by changing the type of probe to use. The choice of a specific form of $\hat{\mathcal{H}}$ thus has to be considered part of our scheme, whose crucial target is the determination of the parameters characterizing the environment $\mathcal{B}$. Clearly *all* assumptions made, with the

 ©2010 The American Physical Society

exception of the Markovian nature of the environment, can be *relaxed*. This insensitivity to stringent conditions and clear general applicability make the scheme experimentally appealing as well as fundamentally interesting. To illustrate the main point of our analysis, we study a general anisotropic Heisenberg model. (In Ref. [8] we discuss the case of a second interesting coupling mechanism, thus showing generality of our results.) We thus take the Hamiltonian $\hat{\mathcal{H}} = \hat{\mathcal{H}}_{xy} + \hat{\mathcal{H}}_{\rm Ising}$ with $\hat{\mathcal{H}}_{xy} = \sum_{k=x,y} J_k(\hat{\sigma}_{k,1} \otimes \hat{\sigma}_{k,2})$ and $\hat{\mathcal{H}}_{\rm Ising} = J_z \hat{\sigma}_{z,1} \otimes \hat{\sigma}_{z,2}$. The nonunitary part of the evolution is entirely ascribed to qubit 2, which is exposed to its environment $\mathcal{B}$ that we take to be both dissipative and dephasing. With this in mind, the evolution of the density matrix ϱ of the system is given by the ME $\partial_\tau \varrho = -i[\hat{\mathcal{H}}_t, \varrho] + \mathcal{L}_{\mathcal{B}}(\varrho)$ with $\hat{\mathcal{H}}_t = \hat{\mathcal{H}}_f + \hat{\mathcal{H}}$. The Liouvillian $\hat{\mathcal{L}}_B(\varrho)$ acting on the density matrix ϱ of the system is $\hat{\mathcal{L}}_B(\varrho) = -\Gamma(\overline{n}+1)(\{|e\rangle_2\langle e|,\varrho\} - 2|g\rangle_2\langle e|\varrho|e\rangle_2\langle g|) - \Gamma\overline{n}(\{|g\rangle_2\langle g|,\varrho\} - 2|e\rangle_2\langle g|\varrho|g\rangle_2\langle e|) - 2\gamma(|g\rangle_2\langle g|\varrho|g\rangle_2\langle g| - \{|g\rangle_2\langle g|,\varrho\})$. The first two terms account for dissipation occurring at rate Γ ($\overline{n}$ is the mean thermal occupation number of the environment), while the last term describes dephasing at rate γ. Our Markovian assumption unambiguously sets the form of such nonunitary parts of the ME and leaves us with the task of determining the coefficients γ, $\overline{n}$, and Γ.

The terms involving $J_{x,y}$ can be grouped together so that $\hat{\mathcal{H}}_{xy} = \hat{\sigma}_{+,1}(J\hat{\sigma}_{-,2} + \delta\hat{\sigma}_{+,2}) + \text{h.c.}$ with $J = J_x + J_y$, $\delta = J_x - J_y$, and $\hat{\sigma}_{\pm,j} = (\hat{\sigma}_{x,j} \pm i\hat{\sigma}_{y,j})/2$. For $\delta \neq 0$ we have that $[\hat{\mathcal{H}}, \sum_j \hat{\sigma}_{z,j}] \neq 0$, which prevents conservation of the total number of excitations, making the analysis rather nontrivial. The dynamics of the system is evaluated by projecting the ME onto the elements of the computational basis $\{|gg\rangle, |ge\rangle, |eg\rangle, |ee\rangle\}$. This leaves us with a set of differential equations characterizing the density matrix of the system. We identify a matrix of coefficients Σ such that the equations for the dynamical evolution become $\mathbf{v}(t) = \mathrm{e}^{\Sigma t}\mathbf{v}(0)$ with $\mathbf{v}(t)$ a vector of time-dependent density matrix entries. The steady state thus corresponds to the eigenvector of Σ with zero eigenvalue. For the anisotropic Heisenberg coupling in $\hat{\mathcal{H}}$, this leads to $\varrho_{\mathcal{H}}^{ss} = [\Gamma\tilde{\varrho}_{\mathcal{H}}^{ss} + J^2\delta^2 G N \mathbb{1}]/d_{\mathcal{H}}$, where we have introduced the matrix (written in the computational basis)

$$\tilde{\varrho}_{\mathcal{H}}^{ss} = \tilde{\varrho}_1 \otimes \tilde{\varrho}_2 + N(\mathcal{E}|ge\rangle_{12}\langle eg| + \mathcal{F}|gg\rangle_{12}\langle ee| + \text{h.c.}) \qquad (1)$$

with $\tilde{\varrho}_1 = \mathcal{A}_-|g\rangle_1\langle g| + \mathcal{A}_+|e\rangle_1\langle e|$, $\tilde{\varrho}_2 = [(N+1)|g\rangle_2\langle g| + (N-1)|e\rangle_2\langle e|]/4$, $N = 2\overline{n}+1$, $G = \Gamma N + 2\gamma$ and the frequencies $\Omega = \omega_1 + \omega_2$ and $\bar{\omega} = \omega_1 - \omega_2$. We have used $\mathcal{A}_\pm = (N \mp 1)(G^2 + \bar{\omega}^2)\delta^2 + (N \pm 1)(G^2 + \Omega^2)J^2$, $\mathcal{E} = -i\Gamma J N \delta^2 (G + i\bar{\omega})$, and $\mathcal{F} = i\Gamma J^2 \delta (G + i\Omega)$. Moreover, we have $d_{\mathcal{H}} = N\{\Gamma N[(G^2+\omega^2)\delta^2 + (G^2+\Omega^2)J^2] + 4GJ^2\delta^2\}$. The entanglement within $\varrho_{\mathcal{H}}^{ss}$ thus depends on the trade-off among all these parameters.

We now temporarily divert from the main topic of our study to look at the amount of entanglement in $\tilde{\varrho}_{\mathcal{H}}^{ss}$. This allows us to later ascertain the role, if any, played by entanglement in our environment characterization scheme. As an entanglement measure, we use the bipartite *negativity* $N_{\hat{\mathcal{H}}}(\tau)$. Dynamically, this is evaluated by determining the $\mathbf{v}(\tau)$'s and its value can be compared to the degree of entanglement between the two qubits at their steady state, $N_{\hat{\mathcal{H}}}^{ss}$. Figure 1 shows an example of such a comparison for an environment being both dissipative and dephasing. One would expect the dynamical behavior of entanglement to depend on the initial preparation of the qubits. The preparation of qubit 1 is $(|g\rangle + |e\rangle)_1/\sqrt{2}$ and we consider various (in general mixed) initial states of qubit 2. Figure 1(a) reveals that $N_{\hat{\mathcal{H}}}(\tau)$ is persistent in time, regardless of the initial preparation of qubit 2. An interesting observation is that J_z does not enter the steady state, implying that the Ising part of $\hat{\mathcal{H}}$ does not play a role in the determination of the entanglement properties of the two-qubit systems in the long-time limit, although it quantitatively affects them in a purely dynamical sense as shown in Fig. 1(b). From now on we set this parameter to zero and concentrate on $\hat{\mathcal{H}}_{xy}$, whose features determine the degree of stationary entanglement. The time required by the system to reach its steady state is sensitive to the environmental parameters $(\gamma, \Gamma, \overline{n})$. This can be seen in Figs. 2(a) and 2(b), where the effects of the amplitude- and phase-damping rates on $N_{\hat{\mathcal{H}}}(\tau)$ are studied. Dephasing has a stronger effect than amplitude damping on

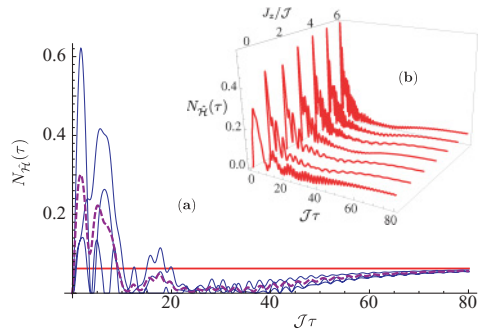

FIG. 1. (Color online) (a) Entanglement against the rescaled interaction time $\mathcal{J}\tau$ for $\Gamma/\mathcal{J} = 0.1$, $\overline{n} = 0$, $\gamma/\mathcal{J} = 10^{-3}$, $J/\mathcal{J} = 0.3$, $\delta/\mathcal{J} = 0.1$, and $J_z = J$ (where $\mathcal{J}$ is the typical order of magnitude of the parameters and depends on the implementation of the scheme). The straight line shows steady-state entanglement while each curve refers to one of three random mixed states of qubit 2. Qubit 1 is prepared in $(|g\rangle + |e\rangle)_1/\sqrt{2}$. The dashed line is the average entanglement calculated over 1000 initial states of qubit 2. (b) Influence of the Ising term in $\hat{\mathcal{H}}$. Each curve shows the average entanglement for increasing J_z [other parameters as in (a)].

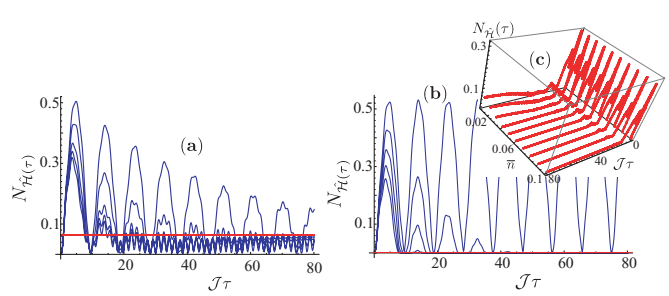

FIG. 2. (Color online) (a) $N_{\hat{\mathcal{H}}}(\tau)$ vs $\mathcal{J}\tau$ (solid line) for $J/\mathcal{J} = 0.3$, $\delta/\mathcal{J} = 0.1$, $\bar{\omega} = 0.3$, $\Omega/\mathcal{J} = 3$, $\gamma/\mathcal{J} = 0.001$, and $\overline{n} = 10^{-3}$. Each line shows the average entanglement for a uniformly random ensemble taken as described earlier, for a set value of $\Gamma \in [0,0.1]\mathcal{J}$, varying in steps of $0.02\mathcal{J}$. The straight line shows $N_{\hat{\mathcal{H}}}^{ss}$. (b) Same as in (a) but for $\Gamma = 0$ and $\gamma \in [0,0.01]\mathcal{J}$, varying in steps of $2 \times 10^{-3}\mathcal{J}$. (c) Effects of thermal mean occupation number $\overline{n}$ of the environment. We plot $N_{\hat{\mathcal{H}}}(\tau)$ vs $\mathcal{J}\tau$ and $\overline{n} \in [0,0.1]$ for $\Gamma/\mathcal{J} = 10^{-3}$.

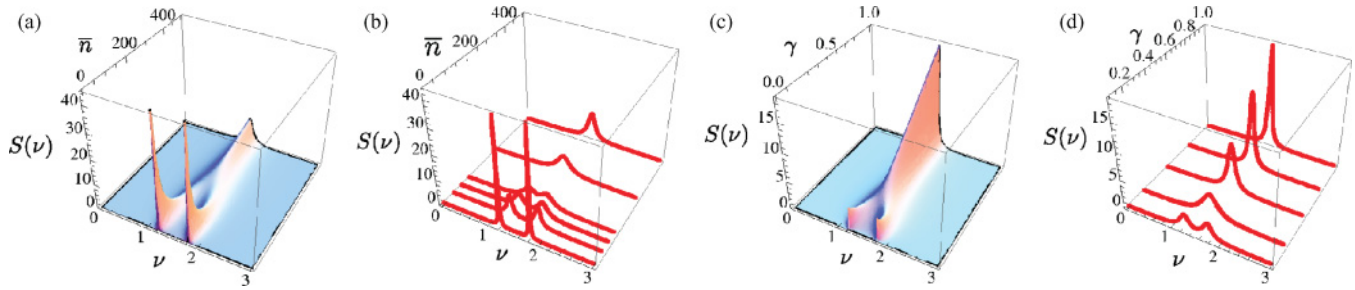

FIG. 3. (Color online) (a) Spectrum $S(\nu)$ of qubit 1 vs ν and the environment mean occupation number $\overline{n}$ for $J/\mathcal{J} = 0.3$, $\delta/\mathcal{J} = 0.1$, $\bar{\omega} = 0$, $\gamma = \Gamma = 10^{-3}\mathcal{J}$, $\Omega/\mathcal{J} = 3$. (b) For a set value of $\overline{n}$, $S(\nu)$ is well approximated by the sum of two Lorentzian functions. Each (red) curve is the result of a best fit over $S(\nu)$ for $\overline{n} = 10$, 60, 100, 140, 300, and 500. (c) $S(\nu)$ vs the frequency ν and the dephasing rate γ for $\overline{n} = 0$, $J/\mathcal{J} = 0.3$, $\delta/\mathcal{J} = 0.1$, $\bar{\omega} = 0$, $\Gamma/\mathcal{J} = 10^{-3}$, and $\Omega/\mathcal{J} = 3$. (d) As for panel (b) for a set value of γ each (red) curve is the best fit for $S(\nu)$ corresponding to $\gamma = 0.1$, 0.25, 0.5, 0.75, and 1.

the settlement of steady entanglement. These considerations help us to understand the results of the environment-probing part of our study, which we now discuss. Motivated by similar recent experimental efforts [1,4], we consider the emission spectrum of qubit 1 in order to discern the effect of the coupling between qubit 2 and $\mathcal{B}$. That is, we aim at determining [13] $S(\nu) = \mathrm{Re}\int d\tau e^{i\nu\tau}\langle\hat{\sigma}_{+,1}(\tau)\hat{\sigma}_{-,1}(0)\rangle_{ss}$, where Re indicates real part; $S(\nu)$ is the Fourier transform of the two-time correlation function $\langle\hat{\sigma}_{+,1}(\tau)\hat{\sigma}_{-,1}(0)\rangle_{ss}$ at the steady state. The linearity of the Bloch-like equations allows the use of the quantum regression theorem to obtain the two-time correlation function we need [13]. The Fourier transform $S(\nu)$ can be given in a fully (although lengthy) analytical form, which we omit. However, we find that the determination of the parameters characterizing the environment affecting qubit 2 is possible by studying $S(\nu)$. Let us illustrate this claim with some instructive situations. Figure 3(a) addresses the case of $\omega_1 = \omega_2$. Both dissipation and dephasing are considered and the spectrum is studied against the thermal occupation number $\overline{n}$ of the bath affecting qubit 2. Two Lorentzian peaks appear at $\overline{n} \ll 1$, centered at $J \pm \sqrt{\delta^2 + \omega_c^2}$, which is a clear effect of quantum interference, still possible in such a quasiunitary situation in virtue of the weak effects of the environment. As soon as the thermal nature of the bath affecting qubit 2 becomes stronger, the incoherent dynamics reduces the distance between the peaks and merges them into a single thermal peak at ω_c. The separation between the Lorentzian functions at $\overline{n} = 0$ gives a direct estimate of the coherent interaction strength, reinforcing the idea that the two-peak structure arises because of strong coherences in the system. For $\omega_1 \neq \omega_2$ and $\overline{n} = 0$, the coherent peaks are located at $\nu_\pm = \frac{1}{2}|\sqrt{4J^2 + \omega^2} \pm \sqrt{4\delta^2 + \Omega^2}|$ for small damping and dephasing, with a nonlinear dependence on Γ, $\overline{n}$, and/or γ. Both the amplitude and the width of the structures involved in $S(\nu)$ depend on Γ almost linearly in the range $\Gamma/\mathcal{J} \in [0,1]$, while the dephasing rate γ has strong effects on the peak-merging process. At small temperatures, increasing γ destroys the interference effect quickly due to cancellation of the off-diagonal elements in $\varrho^{ss}_{\hat{\mathcal{H}}}$ [see Fig. 3(c)], while increasing the dissipation rate leads to a decrease in the amplitude of the peaks. Hence, the engineered interaction allows us to identify the characteristics of the environment affecting qubit 2. We can thus conclude that the analysis of the spectrum $S(\nu)$ of qubit 1 is able to provide full information on the details of the open-system dynamics experienced by qubit 2. The shape, height, width, and structure of $S(\nu)$ can be compared to data acquired experimentally. By simply fitting such data with our analytic formulas, one can give excellent estimates of the environmental features.

Although the spectrum is the most powerful diagnostic tool in our investigation, its form makes it difficult to get an immediate idea of the orders of magnitude of the parameters being involved in the dynamics at hand. In light of our previous discussions, this information can instead be easily gathered by approximating the spectra shown in Figs. 3(a) and 3(c) with the sum of two Lorentzian functions, whose respective maxima get closer as the characteristic parameters of the environmental effects are allowed to grow. We have thus checked that a reliable characterization of $S(\nu)$ is achieved by means of the fitting function $S_{\mathrm{fit}}(\nu) = \sum_{j=l,r} A_j/[B_j + (\nu - \nu_j^0)^2]$, where label j identifies the leftmost and rightmost Lorentzian, while A_j, B_j, and ν_j^0 depend, in general, on the sets of parameters of the dynamics (coherent and incoherent). For instance, at $\overline{n} = 0$ and for $\gamma, \Gamma \ll \mathcal{J}$, we expect that $\nu_l^0 = \nu_-$ ($\nu_r^0 = \nu_+$). Moreover, $2\sqrt{B_j}$ gives the width of each Lorentzian, whose maximum is given by A_j/B_j. As shown in Figs. 3(a), 3(c), and 4, we have found an excellent agreement between the exact analytic expression of $S(\nu)$ and its fitting function. Moreover, it allows us to draw an analogy between the behavior of $S(\nu)$ highlighted here and what occurs for the well-known

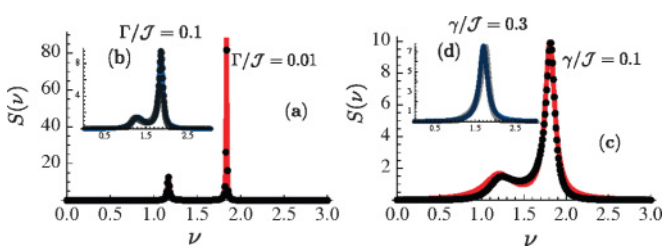

FIG. 4. (Color online) (a, b) The dots show the behavior of $S(\nu)$ for an amplitude-damping-like channel with $\gamma = 0$ and $\Gamma/\mathcal{J} = 0.01$ and 0.1 for $J/\mathcal{J} = 0.3$, $\delta/\mathcal{J} = 0.1$, $\overline{\omega}/\mathcal{J} = 0.3$, and $\overline{n} = 1$. Each solid line is a fit to the sum of two Lorentzian functions having features analogous to those discussed earlier. The agreement between the analytic function and the fitting one is excellent. (c, d): Same as panels (a) and (b) but for $\Gamma = 0$ and $\gamma/\mathcal{J} = 0.1$ and 0.3.

Autler-Townes doublets [14] found for a multilevel atom strongly interacting with an electromagnetic field. In this latter case, the atomic spectrum of emission consists of two split Lorentzian peaks with width proportional to the spontaneous emission rate of the atom, in full similarity with what is found and discussed in our study. As soon as the incoherent atomic emission dominates over the coherent interaction with the field, the Autler-Townes doublet disappears in favor of an incoherent, single-peak structure, which again is strongly reminiscent of what we find for the behavior of $S(\nu)$ under increasingly stronger environmental effects. The qualitative similarities that could be seen by inspection of the figures presented here are made more rigorous by the use of the two-Lorentzian structure given in $S_{\rm fit}(\nu)$. In fact, this allows us to infer, for instance, the rate Γ or the occupation number $\overline{n}$ of the environment. A general analytic expression for the width of the peaks in $S(\nu)$ is not in order, as it results from the solution of a eighth-order algebraic equation in ν. However, interesting insight can still be gained. For the sake of definiteness, let us concentrate on the large $\overline{n}$ limit, which is somehow easier to describe. By assigning the values of Γ and γ, one numerically finds an inverse dependence of the full width at half maximum (FWHM) of the Lorentzian peak in $S(\nu)$ on $\overline{n}$. In fact, an excellent fitting of the analytical curve is obtained by using the model $\mathrm{FWHM}(\overline{n}) = \alpha[\beta + (\overline{n}+1)]^{-1}$, where α and β are two functions of the remaining parameters in the problem. This allows one to determine the temperature of $\mathcal{B}$ by postprocessing the experimental data acquired on $S(\nu)$. The other parameters can be similarly determined. A completely analogous approach can be taken in order to assess the case of multilevel systems to be probed, up to continuous variable ones. In Ref. [8] we discuss an example of such an instance that proves how the validity of our approach goes beyond the scenario discussed here.

Finally, we make an important remark: the presence of nonclassical correlations between the probed and probing systems is not relevant to the characterization process described here. In fact, for the case of Fig. 3(a), $\varrho_{\mathcal{H}}^{ss}$ is separable already at $\overline{n} \sim 0.1$, while the discrimination of the properties of $\mathcal{B}$ is still possible. For $\overline{n} \gtrsim 1$, $\varrho_{\mathcal{H}}^{ss}$ has nonzero (although small) coherences, giving witness to the existence of classical correlations between the two qubits. This can be seen by showing that the corresponding mutual information of the steady state (which accounts for both classical and quantum correlations) is non-null, implying that the "mixedness" of the state of qubit 1 is due not to the entanglement involving the inaccessible part but to the shared effects arising from the presence of an environment, which are the features probed by $S(\nu)$. While the possibility of characterizing an environment even in the absence of entanglement can be understood using arguments based on the no-signaling theorem [9], this result allows us to draw a fundamentally interesting conclusion: environmental characterization is possible as long as a proper correlation-establishing interaction with a probe is present. The noncentral role played by entanglement in our scheme already sets it apart from many previous proposals. It should also be stressed that the scheme presented has, in effect, already been experimentally realized for continuous-variable systems [8], making it immediately useful in the current experimental field. A surprising point here is that the information about the open dynamics of the inaccessible system can be inferred just by probing the *steady state* of the ancilla. The clear general applicability of our protocol to effectively any situation in which a Markovian assumption can be made makes our results both pragmatically relevant and fundamentally interesting.

We acknowledge support from Department for Employment and Learning (DEL), the UK Engineering and Physical Sciences Research Council (EPSRC), the Quantum Information Processing Interdisciplinary Research Collaboration, the Royal Society, and the Wolfson Foundation. M.P. thanks the EPSRC (Grant No. EP/G004579/1) for support.

[1] A. Wallraff *et al.*, Nature (London) **431**, 162 (2004); D. I. Schuster *et al.*, *ibid.* **445**, 515 (2007).

[2] F. H. L. Koppens *et al.*, Nature (London) **442**, 766 (2006).

[3] M. D. LaHaye *et al.*, Science **304**, 74 (2004); A. Naik *et al.*, Nature (London) **443**, 193 (2006).

[4] T. J. Kippenberg and K. J. Vahala, Science **321**, 1172 (2008); F. Marquardt and S. M. Girvin, e-print arXiv:0905.0566.

[5] J. Park *et al.*, Nature (London) **417**, 722 (2002); L. Venkataraman *et al.*, *ibid.* **442**, 904 (2006).

[6] M. Greiner *et al.*, Nature (London) **415**, 39 (2002).

[7] D. Burgarth, K. Maruyama, and F. Nori, Phys. Rev. A **79**, 020305(R) (2009); C. Di Franco, M. Paternostro, and M. S. Kim, Phys. Rev. Lett. **102**, 187203 (2009).

[8] See supplementary material at [http://link.aps.org/supplemental/10.1103/PhysRevA.81.050301].

[9] D. Deutsch and P. Hayden, Proc. R. Soc. London Sect. A **456**, 1759 (1999).

[10] N. P. Oxtoby *et al.*, New J. Phys. **11**, 063028 (2009).

[11] S. De Liberato, Phys. Rev. A **76**, 042107 (2007).

[12] I. Rau, G. Johansson, and A. Shnirman, Phys. Rev. B **70**, 054521 (2004). The non-Markovian environment is currently under study [S. Campbell *et al.* (unpublished)].

[13] P. Meystre and M. Sargent III, *Elements of Quantum Optics* (Springer, Heidelberg, 1990). Given the operators $\{\hat{O}_j\}$ obeying the equations $\partial_\tau \langle \hat{O}_i(\tau)\rangle = \sum_j M_{ij}\langle \hat{O}_j(\tau)\rangle$ with $\mathbf{M}$ a squared matrix, the quantum regression theorem states that the correlations $\langle \hat{O}_i(\tau)\hat{O}_k(0)\rangle$ satisfy the equations $\{\tilde{\mathbf{C}}(s) = (s\mathbb{1}-\mathbf{M})^{-1}\tilde{\mathbf{C}}(0)$ with $\tilde{\mathbf{C}}(s)$ the Laplace transform of vector $\mathbf{C}(\tau)$ whose elements are given by the properly ordered $\langle \hat{O}_i(\tau)\hat{O}_k(0)\rangle_{ss}$'s. By arranging $\mathbf{C}(\tau)$ so that its first element is $\langle \hat{\sigma}_{+,1}(\tau)\hat{\sigma}_{-,1}(0)\rangle_{ss}$, we arrive at$\}$ $S(\nu) = \mathrm{Re}[(i\nu\mathbb{1}-\mathbf{M})^{-1}\mathbf{C}(0)]_1$. $\mathbf{M}$ is extracted from the differential equations for the two-time correlation functions.

[14] S. H. Autler and C. H. Townes, Phys. Rev. **100**, 703 (1955).